ARCHIVES OF ACOUSTICS
11, 3, 299-312 (1986)

AN ACOUSTIC MICROSCOPE IN MEASUREMENTS OF MECHANICAL PROPERTIES OF SURFACE LAYERS — $V(z)$

JERZY LITNIEWSKI

Department of Ultrasonics, Institute of Fundamental Technological Research,
Polish Academy of Sciences
(00-049 Warsaw, ul. Świętokrzyska 21)

The $V(z)$ measuring technique, i.e. the application of the acoustic microscope as a measurement tool is presented and explained. In the measurements, the pressure amplitude distribution on the surface of the lens is controlled in a certain range, enabling $V(z)$ curves to be optimized with respect to oscillation amplitudes obtained for the given material.

$V(z)$ curves obtained with this set-up and calculated from them Rayleigh wave velocities are included in the paper. The possibility of using such a set-up in thin film measurements has been pointed out.

1. Introduction

The $V(z)$ measurement technique has been developed parallely with acoustic microscopy [1, 2]. First investigations have been conducted independently by A. Atalar at the university in Stanford and R. G. Wilson in Hughes [3, 4]. This technique applies the acoustic microscope which acts in reflection mode.

A strongly focused beam of ultrasounds (frequency 20 MHz — 100 GHz) is reflected from a sample located in the focal plane, returns to the piezoelectronic transducer and induces an electric signal, which controls the brightness of the spot on the screen [5, 6]. The sample is scanned in the XY plane and the location of the focal point on the sample is correlated with the position of the spot on the screen.

If we stop XY scanning and the distance along the Z-axis will be changed, i.e. the distance between the sample and the lens, then the voltage on the transducer proves to depend strongly on this distance. Graphs of voltage in terms of the lenssample distance have been called $V(z)$ curves. The $V(z)$ curve for a distance z, between the focal point of the lens and the radius of curvature of the lens seems particularily interesting. In this range, the oscillation period of $V(z)$ curves is velocity-dependent and the amplitude is dependent on the attenuation of Rayleigh waves, which can propagate on the surface of the sample. Therefore, $V(z)$ curves are called "acoustic material signature", because they univocally characterize the investigated material.

Leading research centres conduct work on the utilization of the $V(z)$ technique in many fields of science, such as:

– measurements of velocity and attenuation of surface waves [7, 8, 9],

– film thickness measurements [10, 11],

– crystal acoustic anisotropy investigations [12],

– detection of subsurface cracks [13],

– measurements of rates of surface hardening [14],

– investigations of the influence of heat treatment on the surface [14],

– measurements of residual stress patterns [15],

– determination of surface distribution of the coefficient of reflection [16, 17],

– acoustic parameter distribution measurements in living cells [18].

Theoretical and experimental research of the process of forming of $V(z)$ curves can lead to the interpretation of images obtained in the acoustic microscope. However, although acoustic microscope technology is highly advanced and microscope images of various materials and biologic samples are being obtained, this problem has not been solved yet.

In our case the lens is located in the near field of the transducer, what through frequency tuning of the sending-receiving transducer enables changes of the pressure amplitude distribution on the lens surface, and thus the optimization of the $V(z)$ curve in terms of the oscillation amplitude.

2. Physical interpretation of the $V(z)$ curve forming effect

W. Parmon and H. L. Bertoni have given the simplest physical interpretation of $V(z)$ forming on basis of the approximation of "geometric acoustics". From among rays reflected directly from the investigated surface (located outside the focal point) only rays near the axis of the system can reach the transducer. At the same time, waves inciding onto the sample under an angle close to the Rayleigh angle induce a *LRW* surface wave (*Leaky Rayleigh Wave*), which propagates on the sample surface and radiates a longitudinal wave under the Rayleigh angle, θ_R, into the liquid. After passing through the lens a part of these waves reach the transducer. The interference of the directly reflected wave and the wave induced by the surface wave occurs on the surface of the transducer. Changes of the distance, z, give rise to a change in the path and phase of the wave, what leads to the oscillations of the $V(z)$ function. The

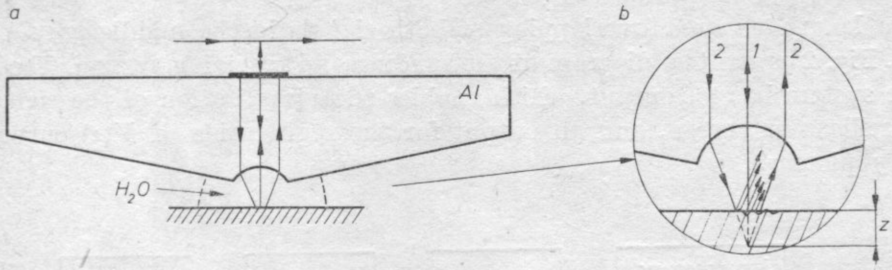

Fig. 1. a) Diagram of the acoustic part of the system for obtaining $V(z)$ curves; b) Diagram of waves composing $V(z)$, i.e. wave directly reflected and wave from *LRW*

oscillation period of the $V(z)$ can be determined on the basis of the given above interpretation. According to the denotation in Fig. 1, the phases of both ray beams can be expressed as follows:

$$\Phi_1 = \Phi_r - \frac{4\pi z}{\lambda_w}, \quad \Phi_2 = \Phi_f - \frac{4\pi z}{\lambda_w \cos\theta_R} + \frac{4\pi z \operatorname{tg}\theta_R}{\lambda_r} + \pi \tag{1}$$

where Φ_f — ray phase for $z = 0$, θ_R — Rayleigh angle $\left(\sin\theta_R = \frac{\lambda_w}{\lambda_R}\right)$, λ_R — Rayleigh wave length, λ_w — wave length in water.

The phase of the wave radiated into water was increased by π according to [20]. The phase difference is:

$$\Phi_1 - \Phi_2 = \frac{4\pi(1-\cos\theta_R)z}{\lambda_R \sin\theta_R} + \pi. \tag{2}$$

The minimum of the $V(z)$ curve is obtained when the phase difference is equal to the π odd multiply. Thus, the calculated $V(z)$ period is:

$$\Delta z = \frac{\lambda_R}{\sin\theta_R}\left(\frac{1+\cos\theta_R}{2}\right). \tag{3}$$

This result is in very good concurrence with experiment.

3. The set-up for obtaining $V(z)$ curves

The experimental set-up built at the Department of Ultrasonics of the IFTR operates in the 30–40 MHz frequency range. Differences in time in which the signal directly reflected from the sample and the signal coming from *LRW* reach the transducer can be derived from eq. (2) for this system. This difference equals 0.2 μs for the reflection from an aluminium sample at a frequency of 36 MHz. Hence, sending pulses of a 1 μs length were used in measurements, because such a length ensured overlapping of both signals in the middle part of the pulse. Fig. 2 presents a diagram of the sending and receiving system. The electronic system has an output, which enables the visualization of the signal on the oscilloscope screen, and an output for the registration of $V(z)$ curves on the xy plotter.

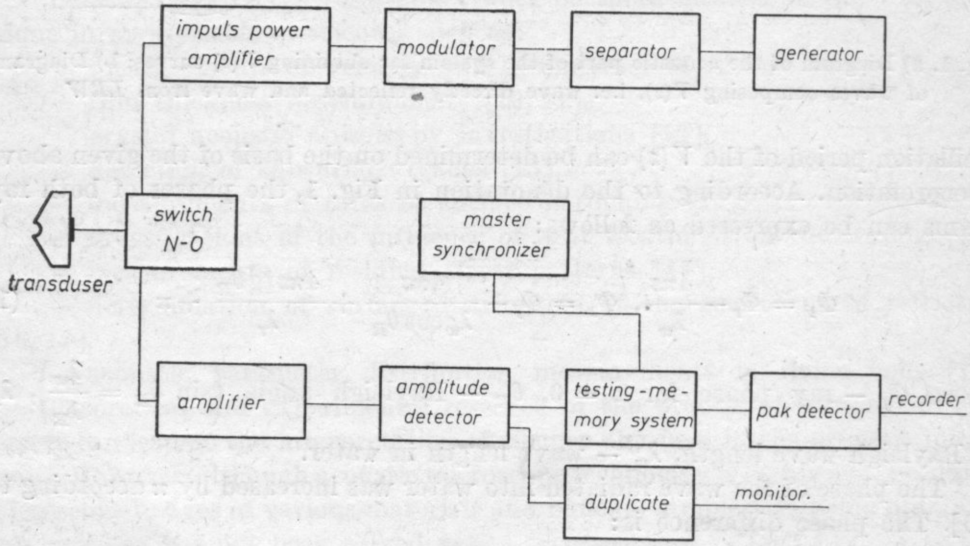

Fig. 2. Diagram of the electronic part of the system for obtaining $V(z)$ curves

The lens with the radius of the spherical cap of 3 mm, was made from aluminium, for which the measured coefficient of damping of a longitudinal wave in this frequency range does not exceed 0.12 dB/cm. Geometrical dimensions of the lens and the whole cylinder were chosen in such a manner that interfering signals reflected from the cylinder walls reached the transducer in a longer time than the signal reflected from the sample. The transducer has a 3 mm radius and the distance between the lens and the transducer equals 22.5 mm. Thus, the lens is situated in the near field of the transducer. When the distance z is changed, then the measured signal moves in a range free from acoustic noise, determined by signals generated by the first and second reflection from the surface of the lens.

The area between the lens and the sample was filled with water. The diameter of the focal point formed by such a system theoretically equals 1.8 wave lengths in water (about 74 μm). The mechanical system ensures sample movement in three directions with the accuracy of setting of 0.01 mm, and the regulation of the inclination of the sample with regard to the axis of the system with the accuracy of 0.5 min.

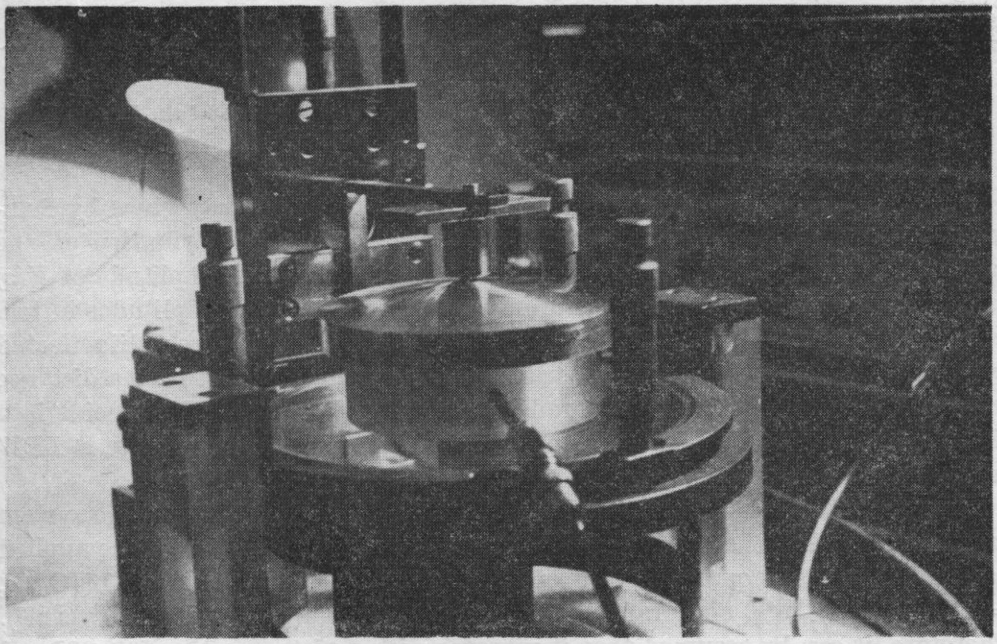

Fig. 3. Photograph of the set-up for obtaining $V(z)$ curves, built at the Department of Ultrasonics IFTR

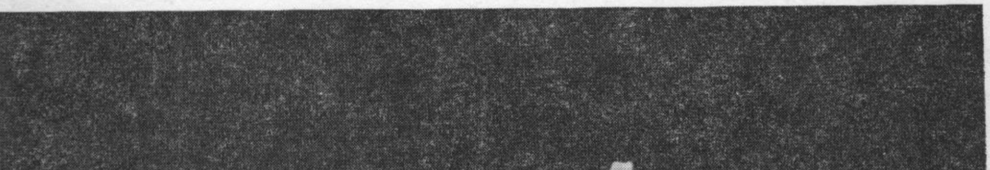

Fig. 4. Photograph of the oscilloscope screen. High frequency signals, from the left: A — sending signal, B — reflection from the lens surface, C — signal reflected from the sample, D — second reflection from the lens surface

4. The influence of the pressure amplitude distribution on the surface of the lens on the oscillation amplitude of $V(z)$ curves

The interpretation of the process of forming of $V(z)$ curves given by PARMON, BERTONI [19] suggests, that the pressure amplitude distribution on the surface of the lens should decisively influence the oscillation amplitude of $V(z)$ curves. Especially, it should depend on the ratio of pressure amplitudes in two regions of the lens — the region near the axis of the system, where radii reflected from the sample directly reach the transducer, and the region at such a distance from the axis of the system, that radii after going through the lens incide into the sample under an angle close to the Rayleigh angle and generate a *LRW* surface wave.

In order to investigate this relationship the spherical surface of the system lens was located in the near field of the transducer. The thickness of the applied here transducer is equal to 1/120 of its diameter. It is made from $LiJO_3$ ($\varrho_c = 18.5 \cdot 10^6$ kg/s m²) and radiates into aluminium ($\varrho_c = 17.3 \cdot 10^6$ kg/s m²). Therefore, it can be assumed that it vibrates with a piston motion [22, 23] and thus calculation results from ZEMANEK'S paper [26] can be applied in this case.

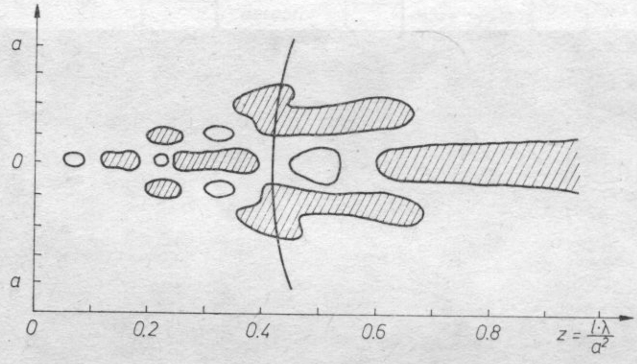

Fig. 5. Pressure amplitude distribution in the near field of the transducer with a radius a, for $a/\lambda = 20$; the position of the lens is denoted. Lined and not lined regions mark places where the pressure amplitude exceeds 0.85 and is below 0.35 of the maximal value of the amplitude, respectively

Fig. 5 presents the theoretical pressure amplitude distribution for a transducer vibrating with a piston motion and with a radius a, and a lens situated in this field [26]. Coordinate $D (D = l\lambda/a^2)$ depends on the product of the wave length λ and the distance from the transducer, l. Hence, changes of the operating frequency of the transducer cause (by changing the distribution of the near field) such changes of the pressure distribution on the surface of the lens, like a displacement of the lens in the near field by a certain distance. Frequency changes between 30 and 40 MHz correspond to changes of coordinate D from 0.4 to 0.55 (Fig. 5).

Phase changes in the pressure distribution on the surface of the lens, due to changes of the operating frequency of the transducer, do not influence the oscillation amplitude of the $V(z)$ curve, because possible additional phase shifts between the wave reflected directly from the sample and the wave from the *LRW* add up with the phase difference generated during the formation of the $V(z)$ curve (2) and thus the $V(z)$ curve is only shifted along the Z-axis without a change in its shape.

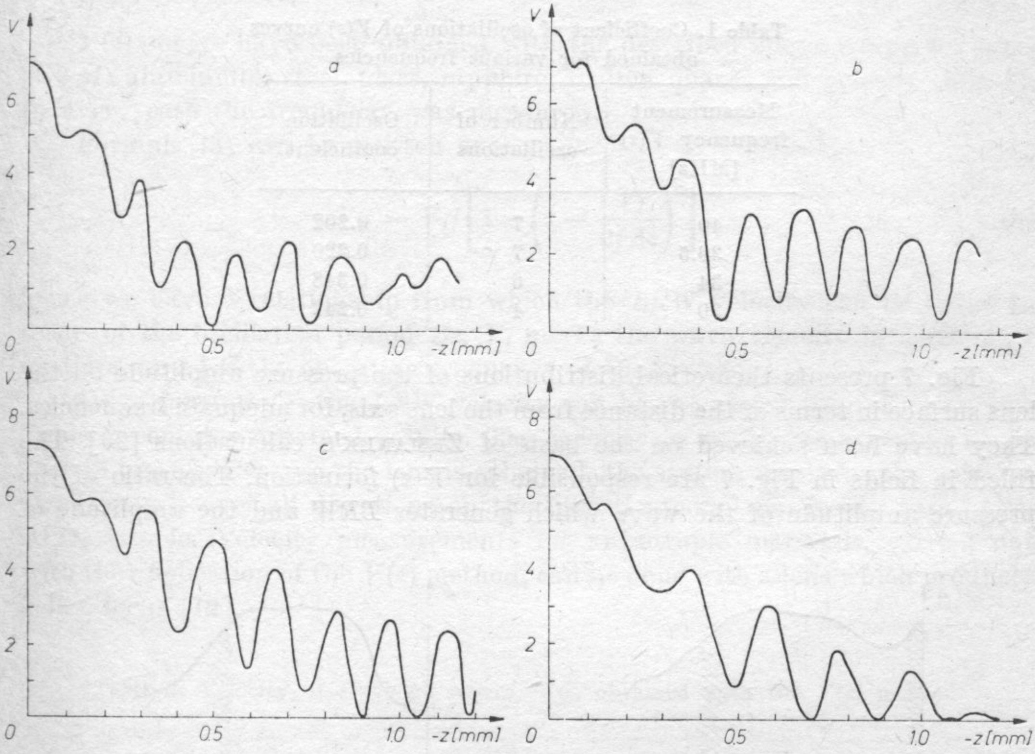

Fig. 6. $V(z)$ curves for an aluminium sample obtained for various frequencies: a) 40 MHz, b) 36.5 MHz, c) 34 MHz, d) 30 MHz

Measurements were performed for four frequencies (30, 34, 36.5, 40 MHz). Fig. 6 presents $V(z)$ curves for an aluminium sample. The coefficient determining the degree of oscillation of the $V(z)$ curve (WO — coefficient of oscillations) has been calculated for every curve. It is defined as the ratio of the mean oscillation amplitude of $V(z)$ to the value of the signal received when the sample is exactly in the focal point.

$$WO = \frac{1}{A_0} \cdot \frac{1}{N} \cdot \sum_{i=1}^{N} A_i \tag{4}$$

where: N — quantity of oscillations, A_i — amplitude of the i-th oscillation, A_0 — amplitude of the voltage from the transducer for a sample in the focal point.

Calculated WO values are given in Table 1.

This coefficient has the maximal value at the frequency of 34 MHz and hence the distribution of the pressure amplitude in this frequency range is optimal for the formation of a $V(z)$ curve.

Table 1. Coefficient of oscillations of $V(z)$ curves obtained for various frequencies

Measurement frequency $V(z)$ [MHz]	Number of oscillations	Oscillation coefficient
40	7	0.202
36.5	7	0.220
34	6	0.348
30	4	0.242

Fig. 7 presents theoretical distributions of the pressure amplitude on the lens surface in terms of the distance from the lens axis, for adequate frequencies. They have been achieved on the basis of ZEMANEK'S calculations [26]. The filled in fields in Fig. 7 are responsible for $V(z)$ formation. The ratio of the pressure amplitude of the wave which generates LRW and the amplitude of

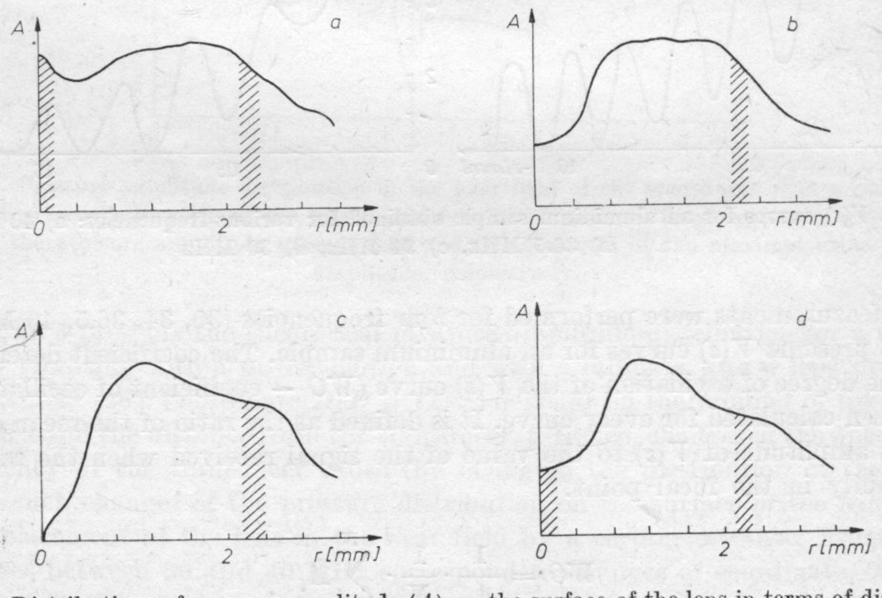

Fig. 7. Distributions of pressure amplitude (A) on the surface of the lens in terms of distance (r) from the axis of the lens, calculated for various frequencies: a) 40 MHz, b) 36.5 MHz, c) 34 MHz, d) 30 MHz

the wave which propagates along the axis is greatest for the frequency of 34 MHz. Because also the maximal oscillation amplitude of $V(z)$ is obtained for this frequency, then such conditions ensure an optimal ratio of the $V(z)$ components, i.e. the wave from the *LRW* and wave reflected directly from the sample.

5. Measurement of surface waves velocities with the $V(z)$ method

$V(z)$ curves have been obtained with the described above set-up for samples of: aluminium, steel, glass, sapphire, molten quartz and perspex (Fig. 8). In every case the frequency was measured.

Formula (3) can be written as:

$$V_R = V_l / \left[1 - \left(1 - \frac{V_l}{2f\Delta z}\right)^2\right]^{1/2} \tag{5}$$

hence we have a relationship from which the *LRW* velocity can be found in terms of the oscillation period Δz. V_l marks the wave velocity in a coupling medium, and f is the operating frequency of the system.

Using formula (5) the *LRW* velocity can be calculated from $V(z)$ curves. Table 2 contains obtained results. The velocity in water was accepted at $V_l = 1.48$ mm/μs. Because the lens is spherical, the system measures the velocity V_r, averaged over all directions on the investigated plane, in the case of an Al_2O_3 sample. Velocity measurements for anisotropic materials, carried out with the application of the $V(z)$ method, can be done with a lens which produces a line-focus [12].

Table 2. Velocity of Rayleigh waves, V_R, obtained with the $V(z)$ method

Material	Number of oscillations	Period of $V(z)$ $[10^{-3}$ m]	V_R calculated $[10^3$m s$^{-1}]$	Measurement accuracy [%]
Aluminium (37.1 MHz)	5	0.150	2.97	3.4
Steel (NC 10) (37.1 MHz)	6	0.158	3.04	2.6
Glass (crown) (37.1 MHz)	4	0.180	3.23	3.1
Molten quartz (33.3 MHz)	3	0.214	3.36	1.5
Al_2O_3C (34.1 MHz)	2	0.535	5.25	4.2
Perspex (35.6 MHz)	3	0.137	2.82	4.3

Interesting results have been obtained for the perspex sample. In this case *LRW* generation does not occur, because the velocity of Rayleigh waves is lower in perspex than in water. So here the lateral wave, which propagates on the water-perspex interface with the velocity of a longitudinal wave in perspex, is responsible for the generation of $V(z)$ curves [24].

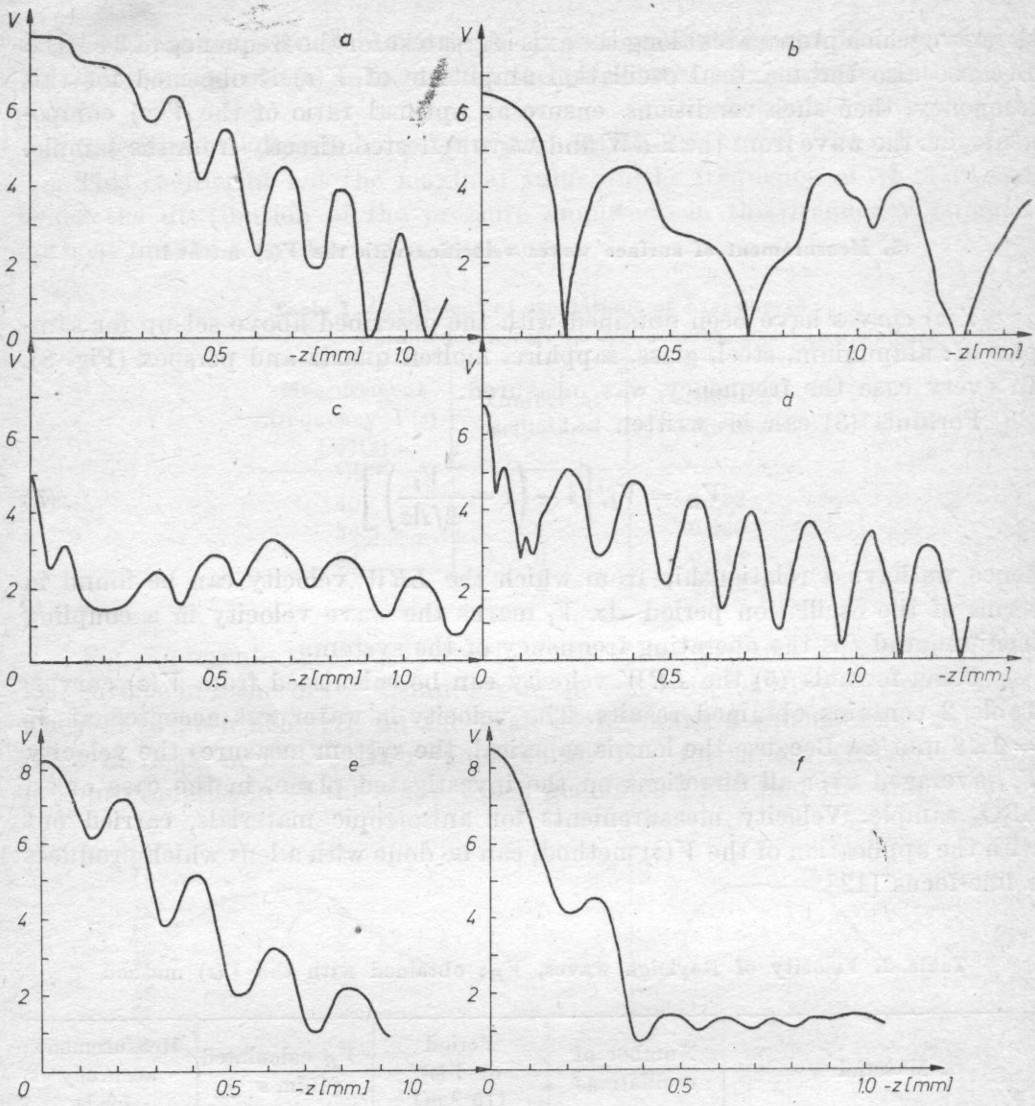

Fig. 8. $V(z)$ curves obtained for a) aluminium, b) Al_2O_3; c) crown-glass, d) steel — NC10, e) molten quartz, f) perspex

The accuracy of obtained results depends mainly on the error in determining the period Δz. An inaccuracy of ± 5 μm in measuring Δz causes a velocity error of 0.1 mm/μs. Additional disturbances are introduced by low-amplitude oscillations, with a period equal to 0.5 wave lengths in water, which overlap $V(z)$. Measuring errors can also result from inaccuracies in setting the sample perpendicularily in respect to the axis of the system.

Very accurate velocity measurements can be done with the application of the numerical technique in finding the oscillation period of $V(z)$, by determining the spectrum of the $V(z)$ function [25].

6. Film thickness measurement with the $V(z)$ method

The $V(z)$ technique also can find application in indirect measurements of the thickness of thin films [10]. To this end the dispersion curve of a surface wave in the film has to be found. Having the relationship between film thickness and surface wave velocity, the film thickness can be determined from velocity measurements.

The following experiment confirms the applicability of the $V(z)$ technique and the built set-up to velocity measurements of surface waves in terms of film thickness.

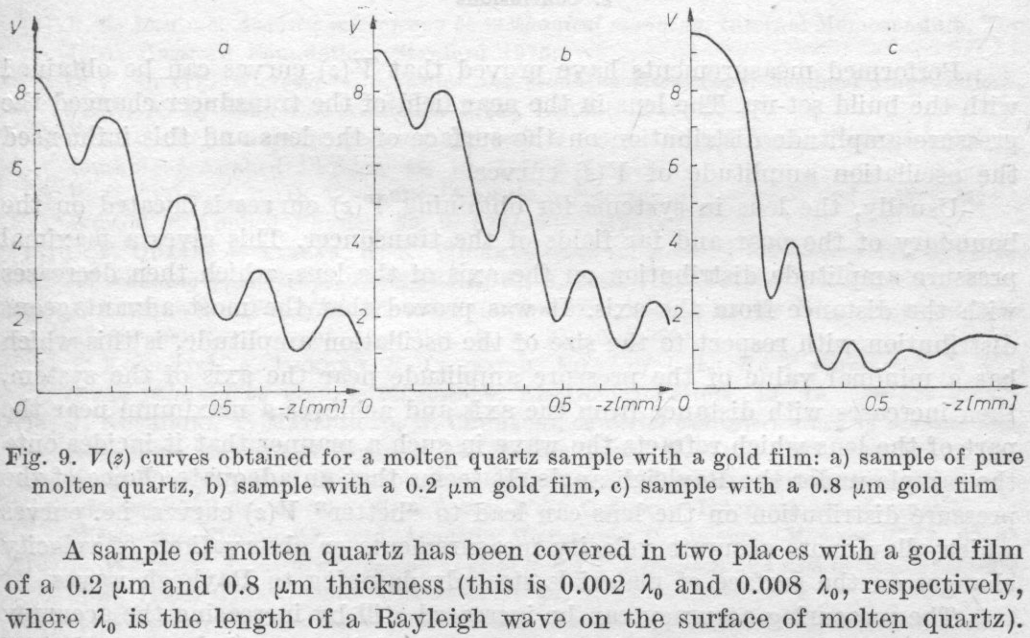

Fig. 9. $V(z)$ curves obtained for a molten quartz sample with a gold film: a) sample of pure molten quartz, b) sample with a 0.2 μm gold film, c) sample with a 0.8 μm gold film

A sample of molten quartz has been covered in two places with a gold film of a 0.2 μm and 0.8 μm thickness (this is 0.002 λ_0 and 0.008 λ_0, respectively, where λ_0 is the length of a Rayleigh wave on the surface of molten quartz). $V(z)$ curves have been obtained for these covered areas and for pure molten quartz. The measurement frequency was optimized and set at 33.3 MHz. The oscillation period of $V(z)$ curves decreased with the increase of thickness. This corresponds to a decrease of the surface wave velocity. The measured oscillation period was used in the calculation of the Rayleigh wave velocity. Table 3 presents the results in terms of film thickness.

A relatively high velocity decrease ($\simeq 5\%$) for a very thin layer of gold (0.002 λ_0) indicates high sensitivity of the method in film thickness measurements. The velocity measuring error for a quartz sample equals about 1.5%. Therefore, the application of this set-up and method should make it possible to observe a gold layer of a 0.0006 λ_0 thickness. This leads to a conclusion that a system with the lens situated in the near field of the transducer is more sensitive than a system with the lens on the boundary of the far and near field [10].

Table 3. Measurement results of *LRW* velocities on a molten quartz sample with a gold film

Gold film thickness $[10^{-6}\ \mathrm{m}(\lambda_0)]$	Oscillation period $[10^{-3}\ \mathrm{m}]$	Calculated velocity $[10^3\ \mathrm{m\ s^{-1}}]$
0	0.214	3.36
0.2 (0.002)	0.192	3.19 95%
0.8 (0.008)	0.163	2.96 88%

7. Conclusions

Performed measurements have proved that $V(z)$ curves can be obtained with the build set-up. The lens in the near field of the transducer changed the pressure amplitude distribution on the surface of the lens and this influenced the oscillation amplitude of $V(z)$ curves.

Usually, the lens in systems for obtaining $V(z)$ curves is located on the boundary of the near and far fields of the transducer. This gives a maximal pressure amplitude distribution on the axis of the lens, which then decreases with the distance from the axis. It was proved that the most advantageous distribution with respect to the size of the oscillation amplitude, is this which has a minimal value of the pressure amplitude near the axis of the system, then increases with distance from the axis and achieves a maximum near the part of the lens which refracts the wave in such a manner that it incides onto the sample under the Rayleigh angle. It seems that an adequate choice of the pressure distribution on the lens can lead to "better" $V(z)$ curves, i.e. curves which allow more accurate velocity measurements or observations of velocity changes on the surface of materials strongly damping to Rayleigh waves.

The measuring accuracy can be increased still by increasing the accuracy of reading of the oscillation period Δz and by obtaining a precisely perpendicular position of the investigated surface in respect to the lens axis.

The greatest advantage of measurements conducted with the $V(z)$ method are results averaged over scarcely ten to twenty wave lengths. Due to this maps of velocity distribution of Rayleigh waves on a given surface can be made.

$V(z)$ curves are sensitive to changes of velocity and damping of surface waves and this causes changes of frequency or oscillation amplitude. Also faults in the investigated material, which interact with the propagating surface wave, should influence $V(z)$ curves. Therefore, the $V(z)$ method is particularily useful in investigations of surface layers of materials.

Acknowledgement

The first in Poland microscope system for ultrasonic investigations by the $V(z)$ method was built at the Department of Ultrasonics IFTR-PAS. This was possible thanks to Prof. L. Filipczyński and Dr. J. Zieniuk as well as Dr. A. Latuszek. The author would also like to thank Doc. S. Turczyński and M. Sc. K. Stypuła for their help in building the electronic part of the system.

References

[1] R. A. LEMONS, *Acoustic microscopy by mechanical scanning*, Internal Memorandum, The J. A. Hartford Foundation, Stanford 1975.

[2] C. F. QUATE, *Microwaves, acoustics and scanning microscopy*, Scanned Image Microscopy, E. A. Ash., Ed. Academic Press, London 1980, 23–55.

[3] A. ATALAR, *An angular spectrum approach to contrast in reflection acoustic microscopy*, Journal of Applied Physics, **49**, 10, 5130–5139 (1978).

[4] R. G. WILSON, R. D. WEGLEIN, *Acoustic microscopy of materials and surface layers*, Journal of Applied Physics, **55**, 9, 3261–3275 (1984).

[5] C. F. QUATE, A. ATALAR, H. K. WICKRAMASINGHE, *Acoustic microscopy with mechanical scanning – a review*, Proc. IEEE, **67**, 8, 1092–1113 (1979).

[6] J. LITNIEWSKI, *The effect of modulation transfer function on the image in an acoustic microscope*, Archives of Acoustics, **8**, 1, 31–40 (1983).

[7] J. KUSHIBIKI, A. OHKUBO, N. CHUBACHI, *Effect of leaky SAW parameters on V(z) curves obtained by acoustic microscopy*, Electronics Letters, **18**, 15, 668–670 (1982).

[8] J. KUSHIBIKI, Y. MATSUMOTO, N. CHUBACHI, *Material characterization by acoustic line-focus beam*, Acoustical Imaging, 13, Plenum Press, N. York 1983, 193–202.

[9] A. A. KULAKOV, A. I. MOROZOV, *Peculiarities of SAW velocity measurements by acoustic microscope*, Proc. of The First Soviet-West Germany International Symposium on Microscope Photometry and Acoustic Microscopy in Science, Moscow 1985, 80–84.

[10] R. WEGLEIN, *Acoustic microscopy applied to SAW dispersion and film thickness measurement*, IEEE Trans. Sonics Ultrason., **SU-27**, 2, 82–86 (1980).

[11] R. WEGLEIN, *Non-destructive film thickness measurement on industrial diamond*, Electronics Letters, **18**, 23, 1003–1004 (1982).

[12] J. KUSHIBIKI, A. OHKUBO, N. CHUBACHI, *Material characterization by acoustic microscope with line-focus beam*, Acoustical Imaging, 12, Plenum Press, N. York 1982, 101–111.

[13] M. G. SOUMEKH, G. A. D. BRIGGS, C. ILETT, *Detection of surfacebreaking cracks in the acoustic microscope*, Acoustical Imaging, 13, Plenum Press, N. York 1983, 119–128.

[14] K. YAMANAKA, Y. ENOMOTO, Y. TSUYA, *Application of scanning acoustic microscope to the study of fracture and wear*, Acoustical Imaging, 12, Plenum Press, N. York 1982, 79–87.

[15] K. LIANG, B. T. KHURI-YAKUB, S. D. BENNETT, G. S. KINO, *Phase measurements in acoustic microscopy*, Proc. Ultrasonics Symposium, Atlanta 1983, **2**, 591–604.

[16] J. A. HILDEBRAND, K. LIANG, S. D. BENNETT, *Fourier transform approach to materials characterization with the acoustic microscope*, Journal of Applied Physics, **54**, 12, 70 16–7019 (1983).

[17] K. K. Liang, G. S. Kino, B. T. Khuri-Yakub, *Material characterization by the inversion of V(z)*, IEEE Trans. on Sonics and Ultrasonics, **SU-32**, 2, 213–224 (1985).

[18] J. A. Hildebrand, D. Ruger, R. N. Johnston, C. F. Quate, *Acoustic microscopy of living cells*, Proc. Nat. Acad. Sci. USA, **78**, 3, 1656–1660 (1981).

[19] W. Parmon, H. L. Bertoni, *Ray interpretation of the material signature in the acoustic microscope*, Electronics Letters, **15**, 21, 684–689 (1979).

[20] H. L. Bertoni, T. Tamir, *Unified theory of Rayleigh-angle phenomena for acoustic beams at liquid-solid interfaces*, Applied Physics, 2, 157–172 (1973).

[21] R. Weglein, *A model for predicting acoustic material signature*, Appl. Phys. Lett. **34**, 3, 179–181 (1979).

[22] G. Łypacewicz, L. Filipczyński, *Measurement method and experimental study of ceramic transducer vibrations*, Acustica, **25**, 1971.

[23] D. Belincourt, D. Curran, H. Jaffe, *Piezoelectric and piezomagnetic materials and their function in transducers*, Physical Acoustics, Academic Press, vol. 1, part A, New York 1964.

[24] L. M. Brekhovskikh, *Waves in Layered Media*, Academic Press, New York 1960.

[25] J. Kushibiki, N. Chubachi, K. Horri, *Velocity measurement of multiple leaky waves on germanium by line-focus-beam acoustic microscope using FFT*, Electronics Letters, **19**, 11, 404–405 (1983).

[26] J. Zemanek, *Beam Behaviour within the Near Field of a Vibrating Piston*, JASA, **49**, 1. 181–191 (1971).

Received on Febraury 5, 1986; revised version on May 25, 1986.